

# Water Vapor Concentration Enhancement in Compressed Humid Nitrogen, Argon, and Carbon Dioxide Measured by Fourier Transform Infrared Spectroscopy<sup>†</sup>

Gerald Koglbauer and Martin Wendland\*

Institut für Verfahrens- und Energietechnik, Universität für Bodenkultur Wien, Muthgasse 107, 1190 Vienna, Austria

Knowledge of the dew point of compressed humid gases is needed for many new technical applications, e.g., compressed air energy storage (CAES), humid air turbine (HAT), or zero emission power plants. A new method was developed to measure the dew point, expressed as vapor concentration enhancement factor, by Fourier transform infrared (FTIR) spectroscopy. This method has already been successfully applied to compressed humid air (Koglbauer and Wendland, *J. Chem. Eng. Data* 2007, 52, 1672–1677). Here, measurements in pure air components were performed at temperatures from (20 to 100) °C and pressures up to 25 MPa for nitrogen and argon and up to 5.5 MPa for carbon dioxide. The estimated combined standard uncertainties (68 % confidence level) of the new experimental data are 0.02 K for temperature, 3.2 kPa for pressure, (0.12 to 1.2) % for the vapor concentration enhancement factor in argon and nitrogen, and (0.5 to 5) % for the vapor concentration enhancement factor in carbon dioxide.

## Introduction

Thermophysical properties of compressed humid gases are needed for, e.g., compressed air energy storage (CAES), carbon dioxide separation and sequestration, and the production, transport, and processing of natural gas. They are classified as an IAPWS Certified Research Need (ICRN-14).<sup>1</sup> An important property is the solubility of water in the compressed gas which increases with the pressure or gas density. This can be described in two different ways:

(a) By the vapor pressure enhancement factor  $f_w$ , which is the ratio of the partial pressure of water  $p_w$  in the saturated compressed humid gas to the vapor pressure  $p_w^0$  of pure water. The partial pressure is usually gained from experimental data of the mole fraction  $x_w$  and the pressure  $p$

$$f_w(T, p) = \frac{p_w}{p_w^0} = x_w \frac{p}{p_w^0} \quad (1)$$

(b) By the vapor concentration enhancement factor  $g_w$ , which is the ratio of the water concentration  $c_w$  (in moles or mass per unit volume) in the saturated compressed humid gas to the saturated vapor density  $c_w^0$  of pure water

$$g_w(T, p) = \frac{c_w}{c_w^0} \quad (2)$$

The relationship between  $f_w$  and  $g_w$  is given by the ratio of the compressibility factors  $Z$  and  $Z_w^0$  of the saturated humid gas or pure water vapor, respectively:

$$g_w = f_w \frac{Z_w^0}{Z} \quad (3)$$

The water content of compressed humid nitrogen, argon, and carbon dioxide has been measured previously either by a flow

apparatus with liquid traps to separate water from gas<sup>2–7</sup> or by the static analytic method with sample valves and analysis by gas chromatography.<sup>8,9</sup> Results of these measurements are given as or can easily be converted to the mole fraction of water  $x_w$  in the vapor phase and yield via eq 1 the vapor pressure enhancement factor  $f_w$ . There are only very limited data available for compressed humid nitrogen<sup>2–4,8</sup> and argon.<sup>3</sup> There are more data on the solubility of water in compressed carbon dioxide (see the reviews by Bamberger et al.<sup>7</sup> and Spycher et al.<sup>10</sup>), but most of them are at pressures where carbon dioxide is a liquid or a supercritical fluid where the water solubility is high and does not reflect the real gas behavior as described by eqs 1 or 2. At real gas conditions,  $f_w$  increases slowly with the pressure; i.e., the mole fraction decreases a little bit slower, as the total pressure increases. Thus, measurements of the mole fraction of water with increasing pressure are very tedious because the amount of gas increases almost proportionally with the pressure while the amount of water stays about the same. Thus, measurements of the mole fraction or of the factor  $f_w$  are very sensitive to errors. A measurement of the water concentration (per unit volume) or  $g_w$  would avoid these problems.

Previously,<sup>11,12</sup> we have developed a new method to measure the vapor concentration enhancement factor  $g_w$  in compressed humid gases by FTIR spectroscopy. The absorbance of IR light by water vapor is very sensitive and increases linearly with the per volume concentration  $c_w$ . This method has been successfully applied to compressed humid air.<sup>11</sup> An apparatus was developed with a high-pressure view cell placed in the sample compartment of an FTIR spectrometer. Equilibrium is achieved in this cell between the gas and a layer of liquid water. Thus, the IR light absorbance could be measured in situ in the saturated gas phase inside the view cell. The vapor concentration enhancement factor  $g_w$  can now be determined rapidly and with good accuracy as a relationship of the absorbance in compressed humid gas to that in saturated pure vapor. An additional calibration in a homogeneous compressed gas sample with known humidity is

<sup>†</sup> Dedicated to Professor Johann Fischer, Vienna, on the occasion of his 65th birthday.

\* Corresponding author. Tel.: +43-1-3709726-212. Fax: +43-1-3709726-210. E-mail: martin.wendland@boku.ac.at.

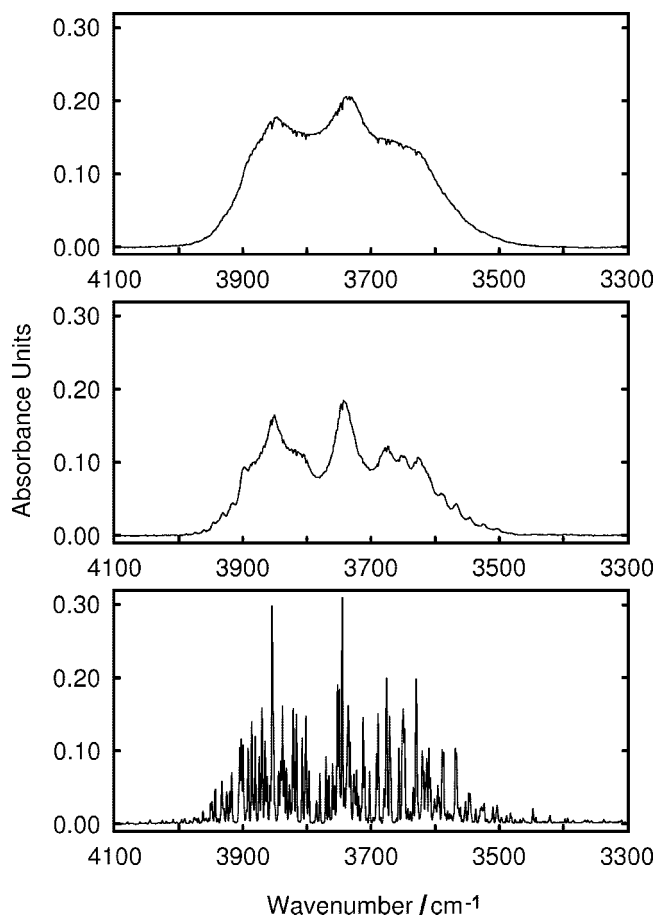


**Figure 1.** Absorbance spectra at  $1\text{ cm}^{-1}$  resolution in saturated compressed humid nitrogen at  $50\text{ }^{\circ}\text{C}$ . From bottom to top: at the vapor pressure of pure water, at 10 MPa, at 25 MPa.

needed to correct for the effect of the gas density on the absorption spectra.

The vapor concentration enhancement factor  $g_w$  in compressed humid nitrogen and argon has been measured at temperatures from (20 to 100)  $^{\circ}\text{C}$  and pressures up to 25 MPa. Furthermore, measurements of  $g_w$  in compressed humid carbon dioxide have been performed at temperatures from (25 to 100)  $^{\circ}\text{C}$  and pressures up to 5.5 MPa.

### Experimental Section

**Chemicals.** Water of p.a. (pro analysi; A.C.S.) grade was purchased from the Merck company (Darmstadt, Germany) with a conductivity of less than  $1\ \mu\text{S}\cdot\text{cm}^{-1}$  at  $25\text{ }^{\circ}\text{C}$ . Nitrogen, argon, and carbon dioxide were delivered by the Linde company (Stadl-Paura, Austria) with volume fraction purities of 99.995 % for carbon dioxide and 99.999 % for nitrogen and argon.

**Method and Apparatus.** The method and apparatus were already described in detail in a previous paper<sup>11</sup> and are summarized here only briefly for the convenience of the reader.

The absorbance  $A$  of IR light by water increases linearly with the water concentration  $c_w$  in the gas phase as described by the Beer–Lambert law. Thus, the vapor concentration enhancement factor can be measured conveniently via the ratio of the absorbance  $A$  in the compressed, saturated gas phase to the absorbance in the pure saturated vapor  $A^0$ :

$$g_w = \frac{c_w}{c_w^0} = \frac{A}{A^0} \cdot \frac{\epsilon^0 d^0}{\epsilon d} = \frac{A}{A^0} \cdot k_\epsilon \quad (4)$$

The linearity constants—the extinction coefficient  $\epsilon$  and the path length  $d$ —are combined to the correction constant  $k_\epsilon$ . The

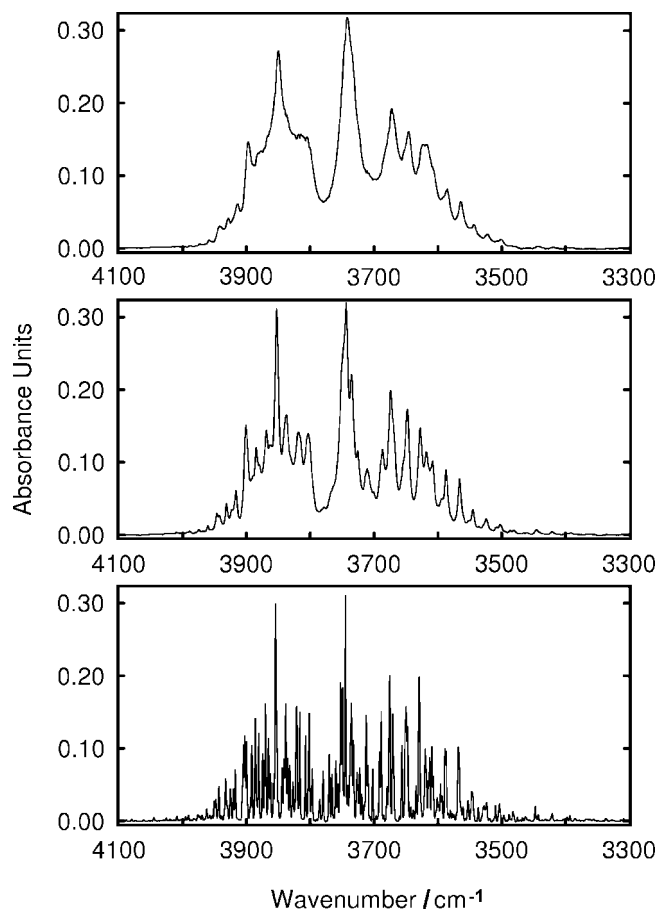


**Figure 2.** Absorbance spectra at  $1\text{ cm}^{-1}$  resolution of saturated compressed humid argon at  $50\text{ }^{\circ}\text{C}$ . From bottom to top: at the vapor pressure of pure water, at 10 MPa, at 25 MPa.

density of the gas has an influence on the extinction coefficient due to peak broadening and complexation between water and the gas molecules. Thus,  $k_\epsilon$  depends on pressure and temperature and is determined at each isotherm as a function of the pressure by calibration in a homogeneous gas sample with known water concentration.

A stainless steel high-pressure view cell was placed in the sample compartment of the FTIR spectrometer. The complete IR light path outside the cell was flushed with nitrogen and dried with a mole sieve. The evacuated view cell was filled with water, and the IR absorbance  $A^0(T)$  of the pure water vapor was measured after equilibration. Then, the sample gas was filled in, and the pressure raised stepwise along an isotherm. After equilibration, the IR absorbance  $A(T, p)$  of the water vapor in the compressed sample gas was measured for each pressure.

**Calibrations and Uncertainties.** The temperature was controlled through a thermostated bath (Gebr. Haake, Karlsruhe, Germany, type N6-B12) and a jacket around the view cell, measured by a  $25\ \Omega$  platinum resistance thermometer (Rosemount, USA, type 162 D) and indicated by a digital resistance bridge (F300, Automatic System Laboratory, UK). The thermometer had been calibrated prior to the measurements according to the International Temperature Scale of 1990 (ITS-90) at three fix points between ( $-40$  and  $156$ )  $^{\circ}\text{C}$  by Landesamt für Mess- und Eichwesen Thüringen (Ilmenau, Germany, uncertainty within  $\pm 2\text{ mK}$ ). The combined standard uncertainty of the temperature measurement was estimated to be within  $\pm 0.02\text{ K}$ . The pressure was measured by a digital piston gauge (Desgranges & Huot, Aubervilliers, France; model 21000 M;

range, (0 to 30) MPa; uncertainty,  $\pm (700 \text{ Pa} + 10.0 \cdot 10^{-5} \text{ p} \cdot \text{Pa}^{-1})$ ). Thus, the maximum uncertainty of the pressure measurement was within  $\pm 3.2 \text{ kPa}$ .

The absorbance  $A$  or  $A^0$  was measured by the FTIR spectrometer (Tensor 27, Bruker Optik GmbH, Ettlingen, Germany) with a standard uncertainty of  $\pm 0.035$  absorbance units ( $u_A$ ). The spectrometric method for nitrogen and argon was identical to the method used for humid air which has been described in detail previously.<sup>11</sup>

Absorbance spectra of water in nitrogen and argon at 50 °C and at saturation are given in Figures 1 and 2. The absorbance spectrum of water in nitrogen changes rapidly with increasing pressure from a typical fingerprint spectrum of pure vapor to a smooth, liquid-like spectrum at 25 MPa. The spectra are very similar to those in compressed humid air.<sup>11,12</sup> The spectrum in nitrogen at 20 MPa is almost identical to the one in air at 25 MPa.<sup>12</sup> Absorbance spectra of water in compressed argon (Figure 2) show different behavior. The thin absorbance peaks at the vapor pressure broaden with increasing pressure and merge partially. This can be attributed to the usual peak broadening with increasing gas density. The liquid-like behavior of the water absorbance bands in compressed air and nitrogen can be attributed to the complexation between water and nitrogen or oxygen molecules.

Carbon dioxide shows a similar, but stronger, effect due to complexation as that for nitrogen and air. Measurements were done below the vapor pressure of carbon dioxide or below 5.5 MPa at 50 °C and higher to avoid liquid or dense supercritical fluid densities. Also, the spectrometric method had to be modified because strong carbon dioxide absorbance bands occur between (3770 and 3530)  $\text{cm}^{-1}$ . Thus, the absorbance spectrum was reduced to the range from (3975 to 3790)  $\text{cm}^{-1}$  for the analysis. Figure 3 shows these reduced water absorbance spectra in compressed carbon dioxide at 50 °C and saturation. A smooth liquid-like behavior already occurs at 5 MPa.

Both peak broadening and complexation have a strong effect on the extinction coefficient and the correction constant  $k_\epsilon$  in eq 4 which has to be determined for each isotherm as a function of pressure by calibration with a known mass of water filled into the cell, which was chosen to be at about 98 % of saturation. Thus, the content of the cell was a homogeneous humid gas with a water concentration which remained constant with increasing pressure. The correction constant could be determined by a simple relation:

$$k_\epsilon = \frac{c_w A^0}{c_w^0 A} = \frac{A^0}{A} \quad (5)$$

For the determination of the factor  $g_w$  with eq 4 and by calibration with eq 5, one measurement of the absorbance  $A$  and one reference measurement of  $A^0$  were needed for both the main measurement of  $g_w$  and the calibration with  $k_\epsilon$ . Additionally, the pressure and the temperature were determined for each measurement of  $A$ , and the temperature only was determined for each measurement of  $A^0$ . The combined standard uncertainty of  $g_w$  can be written with the error propagation law as<sup>11</sup>

$$\frac{\Delta g_w}{g_w} = \sqrt{2\left(\frac{\Delta p}{p}\right)^2 + 4\left(\frac{\Delta T}{T}\right)^2 + 4\left(\frac{\Delta A}{A^0}\right)^2 + \left(\frac{\Delta k_\epsilon^{\text{diff}}}{k_\epsilon}\right)^2 + \left(\frac{\Delta k_\epsilon^{\text{corr}}}{k_\epsilon}\right)^2} \quad (6)$$

Two additional contributions to the uncertainty from the calibration have been included: one contribution from the

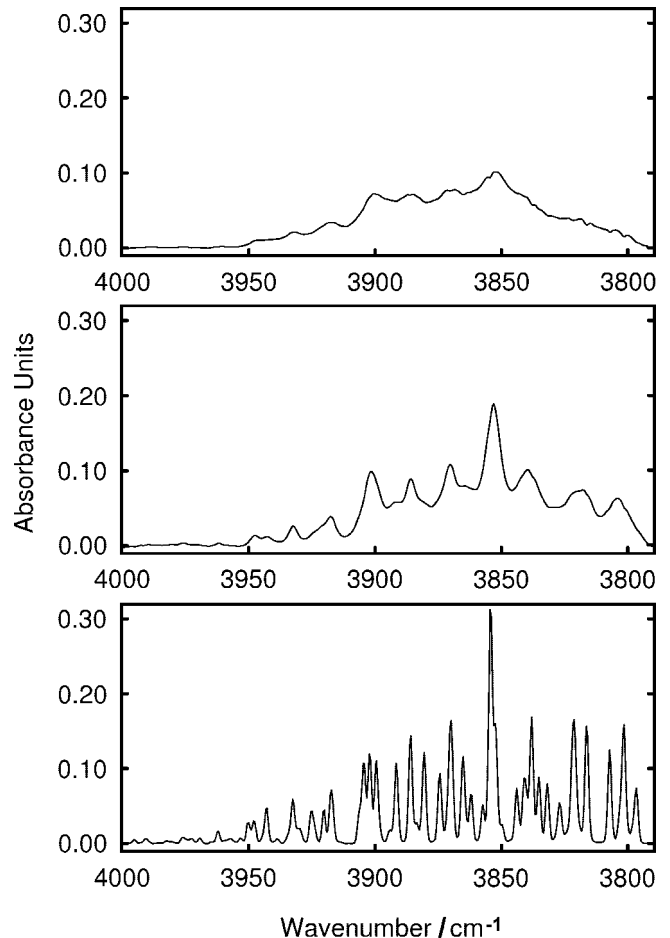


**Figure 3.** Absorbance spectra at 1  $\text{cm}^{-1}$  resolution of saturated compressed humid carbon dioxide at 50 °C. From bottom to top: at the vapor pressure of pure water, at 2.5 MPa, at 5.0 MPa.

diffusion in the 1/16 in. capillary tube that connects the cell to the piston gauge, which can lead to a systematic error in the concentration of the homogeneous humid gas and was determined from nonsteady diffusion to be  $\Delta k_\epsilon^{\text{diff}}/k_\epsilon = 0.04 \%$  for carbon dioxide and 0.06 % for nitrogen and argon, and one contribution from the correlation of  $k_\epsilon$  with fifth-order polynomials that was within  $\Delta k_\epsilon^{\text{corr}}/k_\epsilon = 0.15 \%$  for nitrogen and argon but quite larger for carbon dioxide with  $\Delta k_\epsilon^{\text{corr}}/k_\epsilon = 0.5 \%$ .

The contributions of the temperature and pressure measurement to the uncertainties are almost negligible, and the uncertainty of the absorbance measurement (with  $\Delta A = 0.035 u_A$ ) is the dominant contribution. This yields a relatively large uncertainty at low temperatures (with  $A^0 = 10 u_A$  at 20 °C for nitrogen, air, and argon) and a very low uncertainty at the highest temperature (with  $A^0 = 300 u_A$  at 100 °C for nitrogen, air, and argon). A detailed analysis of the uncertainties was given for compressed humid air in the previous paper.<sup>11</sup> The estimated uncertainties for compressed humid nitrogen and argon are similar to those of air, whereas they are significantly higher for carbon dioxide.

The spectroscopic method used for the compressed humid carbon dioxide system differs from the one used for nitrogen, argon, and air as described above, which yielded higher uncertainties. The reduced spectral range used for the integration resulted in lower absorbance values and hence a higher relative uncertainty  $\Delta A/A$ . Additionally, opposite to the nitrogen, argon, and air measurements, the absorbance  $A(T, p)$  decreased with increasing pressure and carbon dioxide density to 50 % of  $A^0$

**Table 1. Experimental Data for the Vapor Concentration Enhancement Factor  $g_w$  of Compressed Humid Nitrogen<sup>a</sup>**

$p/\text{MPa}$	$g_w$								
	$t = 20\text{ }^\circ\text{C}$	$t = 30\text{ }^\circ\text{C}$	$t = 40\text{ }^\circ\text{C}$	$t = 50\text{ }^\circ\text{C}$	$t = 60\text{ }^\circ\text{C}$	$t = 70\text{ }^\circ\text{C}$	$t = 80\text{ }^\circ\text{C}$	$t = 90\text{ }^\circ\text{C}$	$t = 100\text{ }^\circ\text{C}$
0.1	1.0024	1.0019	1.0055	1.0038	1.0046	1.0045	1.0013	1.0038	—
1.0	1.0405	1.0375	1.0402	1.0354	1.0370	1.0280	1.0200	1.0177	1.0146
2.0	1.0840	1.0973	1.0807	1.0749	1.0730	1.0619	1.0557	1.0438	1.0376
3.5	1.1725	1.1514	1.1489	1.1310	1.1303	1.1073	1.0933	1.0743	1.0634
5.0	1.2313	1.2426	1.2031	1.1923	1.1801	1.1498	1.1263	1.1041	1.0888
7.5	1.3612	1.3401	1.3181	1.2815	1.2701	1.2241	1.1884	1.1535	1.1283
10.0	1.4941	1.4658	1.4208	1.3756	1.3574	1.2949	1.2536	1.2081	1.1753
12.5	1.6252	1.5593	1.5306	1.4665	1.4438	1.3659	1.3177	1.2570	1.2192
15.0	1.7416	1.6951	1.6410	1.5602	1.5302	1.4350	1.3780	1.3086	1.2639
17.5	1.8677	1.8053	1.7421	1.6549	1.6098	1.5083	1.4432	1.3647	1.3082
20.0	1.9829	1.9178	1.8513	1.7462	1.6901	1.5830	1.5070	1.4172	1.3518
22.5	2.0812	2.0360	1.9575	1.8426	1.7663	1.6542	1.5680	1.4626	1.3926
25.0	2.1958	2.1418	2.0544	1.9270	1.8406	1.7139	1.6290	1.5183	1.4396
$\Delta g_w/g_w$	0.0121	0.0074	0.0052	0.0037	0.0027	0.0020	0.0018	0.0017	0.0017

<sup>a</sup> Combined standard uncertainties  $\Delta g_w/g_w$  are given with a 68 % confidence level.**Table 2. Experimental Data for the Vapor Concentration Enhancement Factor  $g_w$  of Compressed Humid Argon<sup>a</sup>**

$p/\text{MPa}$	$g_w$								
	$t = 20\text{ }^\circ\text{C}$	$t = 30\text{ }^\circ\text{C}$	$t = 40\text{ }^\circ\text{C}$	$t = 50\text{ }^\circ\text{C}$	$t = 60\text{ }^\circ\text{C}$	$t = 70\text{ }^\circ\text{C}$	$t = 80\text{ }^\circ\text{C}$	$t = 90\text{ }^\circ\text{C}$	$t = 100\text{ }^\circ\text{C}$
0.1	0.9962	1.0014	1.0037	0.9992	0.9984	1.0034	0.9996	1.0009	—
1.0	1.0241	1.0228	1.0171	1.0150	1.0125	1.0114	1.0142	1.0145	1.0031
2.0	1.0710	1.0497	1.0482	1.0367	1.0303	1.0337	1.0320	1.0291	1.0181
3.5	1.1198	1.0965	1.0813	1.0736	1.0585	1.0581	1.0521	1.0484	1.0435
5.0	1.1584	1.1386	1.1088	1.1028	1.0924	1.0850	1.0751	1.0708	1.0662
7.5	1.2304	1.1973	1.1680	1.1493	1.1347	1.1195	1.1154	1.1072	1.0982
10.0	1.3145	1.2744	1.2257	1.1991	1.1780	1.1593	1.1497	1.1403	1.1310
12.5	1.4008	1.3268	1.2821	1.2542	1.2282	1.1986	1.1847	1.1702	1.1616
15.0	1.4703	1.4120	1.3495	1.3047	1.2772	1.2381	1.2194	1.2013	1.1898
17.5	1.5450	1.4647	1.4118	1.3446	1.3148	1.2799	1.2530	1.2399	1.2186
20.0	1.6066	1.5241	1.4576	1.3997	1.3567	1.3208	1.2870	1.2707	1.2515
22.5	1.6901	1.5880	1.5127	1.4467	1.3923	1.3602	1.3229	1.3032	1.2839
25.0	1.7503	1.6452	1.5615	1.4935	1.4343	1.3922	1.3535	1.3321	1.3107
$\Delta g_w/g_w$	0.0121	0.0074	0.0052	0.0037	0.0027	0.0020	0.0018	0.0017	0.0017

<sup>a</sup> Combined standard uncertainties  $\Delta g_w/g_w$  are given with a 68 % confidence level.**Table 3. Experimental Data for the Vapor Concentration Enhancement Factor  $g_w$  of Compressed Humid Carbon Dioxide<sup>a</sup>**

$p/\text{MPa}$	$g_w$					
	$t = 25\text{ }^\circ\text{C}$	$t = 30\text{ }^\circ\text{C}$	$t = 40\text{ }^\circ\text{C}$	$t = 50\text{ }^\circ\text{C}$	$t = 75\text{ }^\circ\text{C}$	$t = 100\text{ }^\circ\text{C}$
0.1	1.0447	1.0400	1.0460	0.9876	1.0069	—
0.5	1.2161	1.2115	1.1871	1.1261	1.1089	1.0449
1.0	1.4166	1.3719	1.3088	1.2569	1.2032	1.1284
1.5	1.5617	1.5221	1.4081	1.3417	1.2857	1.1789
2.0	1.7071	1.6326	1.4922	1.4325	1.3674	1.2204
2.5	1.8643	1.7225	1.5757	1.5226	1.4357	1.2585
3.0	1.9679	1.8385	1.6394	1.5987	1.5008	1.2946
3.5	2.0771	1.9583	1.7423	1.6577	1.5593	1.3285
4.0	2.1470	2.0718	1.7924	1.7153	1.6305	1.3446
4.5	—	—	1.8536	1.7813	1.7071	1.3680
5.0	—	—	—	1.8444	1.7918	1.4079
5.5	—	—	—	1.8848	1.8502	1.4402
$\Delta g_w/g_w$	0.0500	0.04096	0.0235	0.0160	0.0070	0.0053

<sup>a</sup> Combined standard uncertainties  $\Delta g_w/g_w$  are given with a 68 % confidence level.

at 5 MPa which also yielded a higher  $\Delta A/A$ . This effect and the cutting of the spectra at a point, where the baseline has not been reached, resulted also in higher errors during the calibration, which is reflected in the higher correlation contribution  $\Delta k_\epsilon^{\text{corr}}/k_\epsilon = 0.5\%$ .

## Results and Discussion

The vapor concentration enhancement factor  $g_w$  of compressed humid nitrogen and argon was measured at isotherms between (20 and 100) °C for at least 13 pressure values per isotherm up to 25 MPa. Also, the  $g_w$  of compressed humid carbon dioxide was measured at isotherms between (25 and 100) °C with at least 12 pressure values per isotherm up to 5.5 MPa.

Results of the measurements and the combined standard uncertainties (confidence level 68 %) of these data, estimated with eq 6, are given in Tables 1, 2, and 3. (To achieve the 95 % confidence level, a coverage factor  $k = 2$  must be applied.)

The consistency of the data can be seen from the plots of the experimental  $g_w$  values along isotherms or isobars. The isothermal  $g_w$  data for compressed humid nitrogen and argon increase almost linearly with the pressure as was already observed for compressed humid air.<sup>11</sup> It shows the same consistency along isotherms as the air data and also corresponds well with the experimental uncertainties. Diagrams of  $g_w$  over the pressure are not given here for the nitrogen and argon data because they look very similar to the corresponding diagram

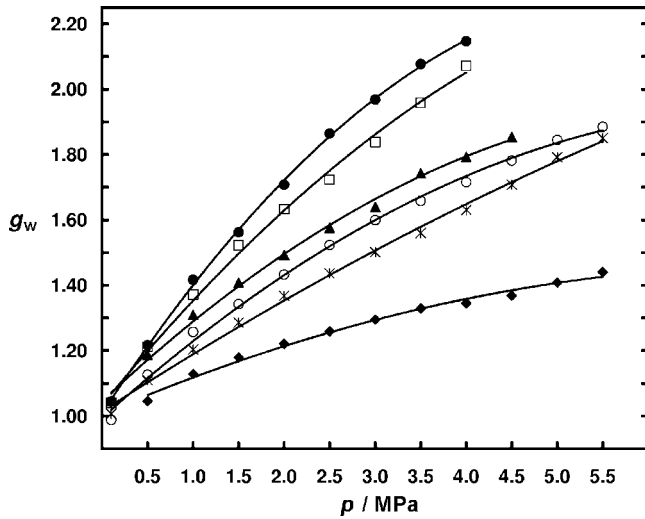


**Figure 4.** Vapor concentration enhancement factor  $g_w$  of compressed humid carbon dioxide. Consistency of the experimental data (points) along isotherms: ●, 25 °C; □, 30 °C; ▲, 40 °C; ○, 50 °C; \*, 75 °C; ◆, 100 °C.

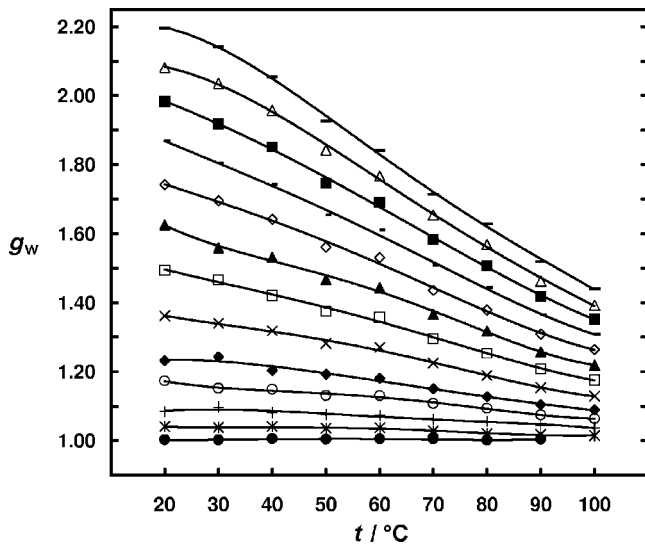


**Figure 5.** Vapor concentration enhancement factor  $g_w$  of compressed humid nitrogen. Consistency of the experimental data (points) along isobars: ●, 0.1 MPa; \*, 1.0 MPa; +, 2.0 MPa; ○, 3.5 MPa; ◆, 5.0 MPa; ×, 7.5 MPa; □, 10.0 MPa; ▲, 12.5 MPa; ◇, 15.0 MPa; -, 17.5 MPa; ■, 20.0 MPa; Δ, 22.5 MPa; —, 25.0 MPa.

for the air data (Figure 5 of the previous paper<sup>11</sup>). Figure 4 shows that the situation is different for compressed humid carbon dioxide. First, isotherms show a curvature which increases with the pressure and results from the more liquid-like densities of the near critical carbon dioxide and the relatively large solubility of carbon dioxide in liquid water. Second, the data are clearly less consistent than the air, nitrogen, and argon data. This corresponds well with the experimental uncertainty of up to 5 %.

In Figures 5 to 7,  $g_w$  is plotted along isobars over the temperature. The data are again very consistent for nitrogen and argon and quite less consistent for carbon dioxide. The nitrogen data in Figure 5 show a very similar behavior to the air data,<sup>11</sup> which is of no surprise because nitrogen is the predominant component in air. Results for compressed humid argon (Figure 6) show quite different behavior of the  $g_w$  values, which decrease steadily with increasing temperature. The data for compressed humid nitrogen and air show a similar steadily

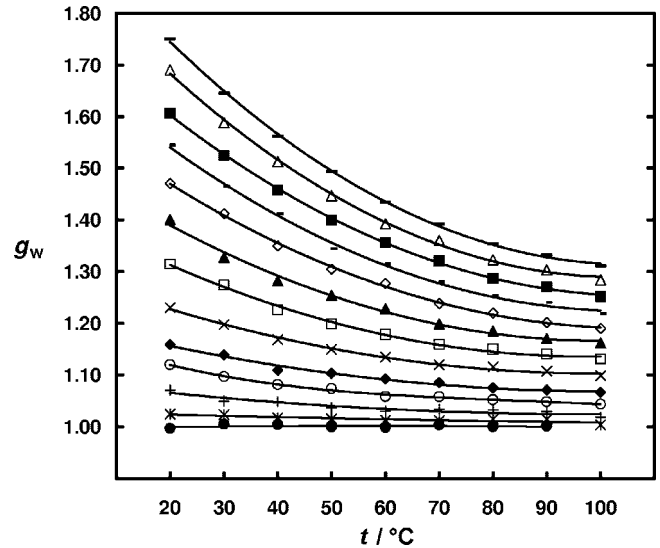


**Figure 6.** Vapor concentration enhancement factor  $g_w$  of compressed humid argon. Consistency of the experimental data (points) along isobars: ●, 0.1 MPa; \*, 1.0; +, 2.0 MPa; ○, 3.5 MPa; ◆, 5.0 MPa; ×, 7.5 MPa; □, 10.0 MPa; ▲, 12.5 MPa; ◇, 15.0 MPa; -, 17.5 MPa; ■, 20.0 MPa; Δ, 22.5; —, 25.0 MPa.

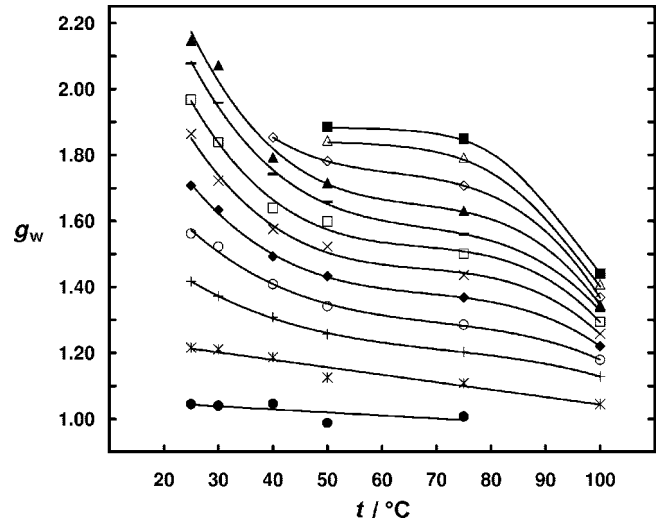


**Figure 7.** Vapor concentration enhancement factor  $g_w$  of compressed humid carbon dioxide. Consistency of the experimental data (points) along isobars: ●, 0.1 MPa; \*, 0.5 MPa; +, 1.0 MPa; ○, 1.5 MPa; ◆, 2.0 MPa; ×, 2.5 MPa; □, 3.0 MPa; -, 3.5 MPa; ▲, 4.0 MPa; ◇, 4.5 MPa; Δ, 5.0 MPa; ■, 5.5 MPa.

decreasing behavior with increasing temperature above about 60 °C but move to a plateau when the temperature decreases toward 20 °C.

The carbon dioxide data in Figure 7 also show a plateau, but now at about (50 to 75) °C. The data now show the usual, steady decrease at lower temperatures. Again, the larger uncertainty of the experimental data of up to 5 % is evident. The consistency of the data, checked by correlation with polynomials is within this uncertainty. We expect that the plateau in the  $g_w$  data, which occurs for compressed humid air and nitrogen at about the same temperature, occurs for carbon dioxide at a higher temperature, and was not observed for argon, is an indication of strong complexation.

No experimental values for the vapor concentration enhancement factor  $g_w$  were found in the literature for compressed humid nitrogen, argon, and carbon dioxide. Only experimental data for the mole fraction  $x_w$  or for quantities which can easily

be converted to mole fraction are available.<sup>2-9</sup> The literature data on these and other compressed humid gases are critically reviewed in a subsequent paper<sup>13</sup> by converting the measured  $x_w$  values to  $f_w$  (eq 1). This review shows for all literature data<sup>2-9</sup> that their consistency in  $f_w$  along isotherms, between different isotherms, and between different sources is much lower than the consistency of the present  $g_w$  data. The data measured by the static analytic method with sample valves and analysis by gas chromatography<sup>8,9</sup> have such a large scattering, when plotted as  $f_w$  over the pressure, that even patterns or tendencies are not observable. Data measured by a flow apparatus<sup>2-7</sup> show a qualitative behavior in  $f_w$  similar to the present  $g_w$  data.<sup>13</sup> A direct comparison of the present  $g_w$  data and the  $f_w$  data from the literature is not possible because an equation of state model would be needed to convert the data with eq 3.

The evidence of complexation between water and nitrogen or oxygen molecules was discussed previously<sup>11</sup> with regard to compressed humid air. Our present work confirms the presence of water–nitrogen and water–carbon dioxide complexes, as already mentioned above by comparing absorbance spectra of compressed humid nitrogen and carbon dioxide (Figures 1 and 3) to those of argon (Figure 2). Kjaergaard et al.<sup>14</sup> calculated the conformations of water–nitrogen and water–oxygen complexes and their infrared activities by ab initio methods. Experimental observations of water–nitrogen complexes<sup>15</sup> by high-resolution IR matrix isolation spectroscopy are also available. Coan and King<sup>6</sup> already presumed the presence of strong carbon dioxide–water complexes and discussed their influence on the solubility of water in carbon dioxide and the second cross virial coefficient of water and carbon dioxide.

## Conclusions

A new method and new apparatus for the measurement of the vapor concentration enhancement factor were applied to compressed humid nitrogen, argon, and carbon dioxide. The new measurements are clearly more consistent than existing data. Thus, a broader and more reliable database is now available for the development of new models for the thermophysical properties of compressed humid gases. There is evidence for complexation of water with nitrogen and carbon dioxide that must be considered for the development of new and improved models.

## Literature Cited

- (1) International Association for the Properties of Water and Steam. IAPWS Certified Research Need - ICRN. Thermophysical Properties of Humid Air and Combustion-Gas Mixtures. ICRN-14, 2002.
- (2) Saddington, A.; Krase, N. W. Vapor–Liquid Equilibria in the System Nitrogen–Water. *J. Am. Chem. Soc.* **1934**, *56*, 353–361.
- (3) Rigby, M.; Prausnitz, J. M. Solubility of Water in Compressed Nitrogen, Argon, and Methane. *J. Phys. Chem.* **1968**, *72*, 330–334.
- (4) Folas, G. K.; Froyna, E. W.; Lovland, J.; Kontogeorgis, G. M.; Solbraa, E. Data and prediction of water content of high pressure nitrogen, methane and natural gas. *Fluid Phase Equilib.* **2007**, *252*, 162–174.
- (5) Wiebe, R.; Gaddy, V. L. Vapor Phase Composition of Carbon Dioxide–Water Mixtures at Various Temperatures and at Pressures to 700 Atmospheres. *J. Am. Chem. Soc.* **1941**, *63*, 475–477.
- (6) Coan, C. R.; King, A. D., Jr. Solubility of Water in Compressed Carbon Dioxide, Nitrous Oxide, and Ethane. Evidence for Hydration of Carbon Dioxide and Nitrous Oxide in the Gas Phase. *J. Am. Chem. Soc.* **1971**, *93*, 1857–1862.
- (7) Bamberger, A.; Sieder, G.; Maurer, G. High-pressure (vapor + liquid) equilibrium in binary mixtures of (carbon dioxide + water or acetic acid) at temperatures from 313 to 353 K. *J. Supercrit. Fluids* **2000**, *17*, 97–110.
- (8) Mohammadi, A. H.; Chapoy, A.; Tohidi, B.; Richon, D. Water Content Measurement and Modelling in the Nitrogen + Water System. *J. Chem. Eng. Data* **2005**, *50*, 241–245.
- (9) Valtz, A.; Chapoy, A.; Coquelet, C.; Paricaud, P.; Richon, D. Vapor-liquid equilibria in the carbon dioxide–water system, measurement and modeling from 278.2 to 318.2 K. *Fluid Phase Equilib.* **2004**, *226*, 333–344.
- (10) Spycher, N.; Pruess, K.; Ennis-King, J. CO<sub>2</sub>-H<sub>2</sub>O mixtures in the geological sequestration of CO<sub>2</sub>. I. Assessment and calculation of mutual solubilities from 12 to 100°C and up to 600 bar. *Geochim. Cosmochim. Acta* **2003**, *67*, 3015–3033.
- (11) Koglbauer, G.; Wendland, M. Water Vapor Concentration Enhancement in Compressed Humid Air Measured by Fourier Transform Infrared Spectroscopy. *J. Chem. Eng. Data* **2007**, *52*, 1672–1677.
- (12) Koglbauer, G. Measurement of Vapor Concentrations in Humid Gases. Ph. D. Thesis at the Universität für Bodenkultur Wien, Vienna, Austria, 2007 (in German).
- (13) Koglbauer, G.; Wendland, M. A Review of Dew Point Measurements in Compressed Humid Gases. **2007**, to be submitted.
- (14) Kjaergaard, H. G.; Low, G. R.; Robinson, T. W.; Howard, D. L. Calculated OH-Stretching Vibrational Transitions in the Water–Nitrogen and Water–Oxygen Complexes. *J. Phys. Chem. A* **2002**, *106*, 8955–8962.
- (15) Coussan, S.; Loutellier, A.; Perchard, J. P.; Racine, S.; Bouteiller, Y. Matrix Isolation Infrared Spectroscopy and DFT Calculations of Complexes between Water and Nitrogen. *J. Mol. Struct.* **1998**, *471*, 37–47.

Received for review July 9, 2007. Accepted October 2, 2007.

JE700386C